2024 IEEE International Conference on Metrology for eXtended Reality, Artificial Intelligence and Neural Engineering (MetroXRAINE) | 979-8-3503-7800-9/24/$31.00 ©2024 IEEE | DOI: 10.1109/METROXRAINE62247.2024.10795901

Multimetric evaluation of knee cartilage degeneration

1st Federica Kiyomi Ciliberti *
Inst. of Biomed and Neural Engineering Reykjavik University)
Reykjavik, Iceland
federica21@ru.is

2nd Ida Maruotto *
Inst. of Biomed and Neural Engineering Reykjavik University
Reykjavik, Iceland
ida23@ru.is

3rd Halldór Jónsson jr
Department of Orthopaedics Landspitali, University Hospital of Iceland
Reykjavik, Iceland
halldor@landspitali.is

4th Magnús Kjartan Gíslason
Inst. of Biomed and Neural Engineering Reykjavik University
Reykjavik, Iceland
magnuskg@ru.is

5th Paolo Gargiulo
Inst. of Biomed and Neural Engineering Reykjavik University
Reykjavik, Iceland
paolo@ru.is

***Abstract*—This study addresses the assessment of knee osteoarthritis (OA), a degenerative joint disease primarily affecting cartilage. While current diagnostic methods like X-rays, CT scans, and MRI scans are subjective, this research aims to develop more objective assessment methods. Focusing on cartilage status in MRI and CT images, the study uses machine learning (ML) techniques to identify predictive parameters for OA severity assessment. Significant differences in cartilage metrics between OA patients and healthy individuals were found. Using the statistical differences a smaller feature set has been extracted and ML analysis (SVM and Logistic Regression) confirmed the effectiveness of these features. This research highlights the importance of precise image analysis and the potential of ML in enhancing OA severity assessment. The emphasis on tibial cartilages aligns with biomechanical considerations, offering insights for personalized treatment approaches.**

***Index Terms*—knee osteoarthritis, medical imaging, segmentation, cartilage, feature selection**

I. Introduction

Osteoarthritis (OA) is a degenerative joint disease involving cartilage, bone, ligaments, and muscles [1]. It primarily manifests as the degradation of cartilage within various joints, leading to pain and reduced mobility. The knee joint is particularly susceptible to OA, significantly impacting the quality of life for affected individuals. Pain in OA is complex, shifting from sporadic weight-bearing discomfort to chronic pain [2] [3]. OA arises from a combination of systemic and local factors. Systemic influences include age, gender (with women being more prone), genetics, and hormonal changes (such as those related to menopause in women) [4]. Local risk factors involve obesity, joint trauma or surgery, repetitive joint stress, physical activity [2], [3], [5], [6]. Moreover, it is a macroalteration that is derived from cells behavior modification [7].

Treatment modalities for knee OA include physical therapy and exercise, medication, injections, and total knee replacement operation in the most severe cases [8]. Therefore, early diagnosis is crucial to timely intervention and potentially avoiding the need for surgery. Assessing the severity of OA presents challenges because of the various classification systems available, each with its own limitations. Early diagnosis remains critical, given the progressive nature of OA, as it allows early intervention with less invasive treatments such as physiotherapy and drug therapy, potentially reducing the need for surgery such as total knee replacement. Therefore, further advances in imaging technology and diagnostic criteria are essential to optimize the management and outcomes of patients with knee OA. Currently, diagnosis of knee OA relies on imaging modalities like X-rays, CT scans, and MRI scans, providing crucial insights into joint damage extent and location. Grading systems such as Ahlbäck and Kellgren-Lawrence scales measure disease severity [9], [10]. However, they may not fully capture clinical symptoms due to subjectivity in interpretation [1]. Given these limitations, there is a need for more quantifiable assessment methods. A combination of CT images and machine learning (ML) approaches have already been used in previous studies on total hip arthroplasty [11]–[13], validating the importance of densitometric features in clinical evaluation. While ML models have also been applied to knee OA studies [14], many of these models are black-box and difficult to interpret. Moreover, these studies typically rely on a single imaging modality, such as X-rays or MRI.

Unlike traditional methods, which often rely on qualitative assessments, this study aims to develop a more objective and quantifiable metric to evaluate knee cartilage status: it uses a cutting-edge combination of imaging modalities and ML algorithms to identify key predictive parameters and image features essential for assessing OA severity. This facilitates faster and better-informed treatment decisions and represents an advancement over existing methods, offering the potential for improved management and outcomes for OA patients.

* These authors (F.K.C. and I.M.) contributed equally

This study is funded by European Union (Horizon 2024 - CORDIS Grant agreement ID: 101057778)

Authorized licensed use limited to: Reykjavik University. Downloaded on November 23,2026 at 11:59:06 UTC from IEEE Xplore. Restrictions apply.

TABLE I: Subjects information

	F	M	age (mean ± std)
D	20	21	62.29 ± 10.19
C	28	24	35.42 ± 13.56

II. Materials & Methods

A. Recruitment

OA-diagnosed patients ('D', Ahlbäck grade 3-4) and healthy control subjects ('C') underwent knee scans, with various characteristics being analyzed. All the subjects were recruited in the context of RESTORE (https://restoreproject.eu/) and SINPAIN (https://www.osteoarthritis-sinpain.eu) EU projects, which aim to find new solutions for knee cartilage regeneration. 93 subjects participated in this study. Part of the cohort scanned both legs in two consecutive acquisitions, for a total of 131 scanned knees (52 belonging to D class, 79 to C). Table I reports all the information about the sex and age of the recruited subjects. An age disparity between groups D and C can be noted: due to the degenerative nature of OA, it is expected that older people are more affected. Although this may introduce some biases in the methodologies used, it is representative of reality.

B. Segmentation and Registration process

The acquired raw images underwent processing utilizing Mimics (Materialise's Interactive Medical Image Control System), a specialized medical imaging software. Segmentation of femoral, lateral tibial, medial tibial, and patellar cartilages was conducted by applying density threshold intervals, followed by additional editing for refinement. This segmentation process was performed on the MRI, since this image modality is suitable for visualizing soft tissues as cartilages. The resulting masks were then converted into highly accurate 3D objects using Mimics.

MRI data are aligned with CT data through image registration, starting from the existing images with the segmentations and 3D objects. Performing the acquisitions in the exact same position ensured accurate superimposition, aided by landmark points selection for alignment. The resultant composite image combined CT with cartilage segmentation derived from MRI. This methodology has already been validated and used in previous researches [15]–[17].

Mimics enabled the determination of radiodensity in Hounsfield units (HU) directly from CT scans. The HU scale provides a quantitative measure of radiodensity. To ensure precise cartilage segmentation, masks were filtered within the 0–300 HU range, excluding areas unrelated to cartilage tissue.

From the registered CT data and corresponding 3D models, various features were extracted, including, for each of the 4 segmented cartilages:

- average of cartilage radiodensity (HU)
- standard deviation (STD) of cartilage radiodensity (HU)
- cartilages volumes (mm^3)
- cartilages surfaces (mm^2)

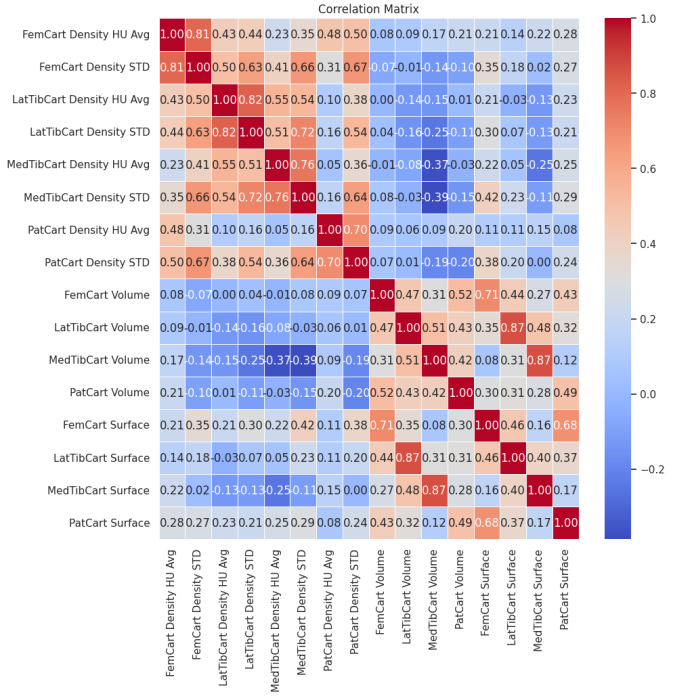

Fig. 1: Correlation Matrix

C. Feature selection

Feature selection aims to obtain a smaller clinically relevant feature set. To do so, we calculate p-values and perform correlation analysis on the features, and they yield a reduced feature set. Moreover, two different artificial intelligence algorithms (SVM and logistic regression) extract machine-relevant features and validate the feature selection. Indeed, these algorithms are trained again with the subset of features to highlight different behaviors or classification accuracies between the sets.

1) Statistical data test: The data have been first analyzed using statistical data analysis. The Shapiro-Wilk test was used to check for normality. Depending on the results, either the t-test or the Mann-Whitney U test was applied to determine if there were statistically significant differences between the means of the control (C) and degenerate (D) groups for each feature. This difference is specified using a p-value < 0.05.

2) Correlation analysis: Correlation analysis determines the strength and direction of the relationship between two variables. The correlation coefficient ranges from -1 to 1; equal to 1 means a perfect positive correlation, equal to -1 means a perfect negative correlation, and 0 means no correlation. The correlation coefficients among the analyzed features are used to exclude from the feature set the feature whose information capacity has already been expressed by other features.

The correlation measures the relation of two variables, and, indeed, our goal in this step is to remove related features that don't provide more information when evaluating the belonging class in addition to the ones already considered.

Authorized licensed use limited to: Reykjavik University. Downloaded on November 23,2026 at 11:59:06 UTC from IEEE Xplore. Restrictions apply.

D. Machine learning

ML analysis allows features to be ranked according to their importance in the classification. The selected algorithms are *Support Vector Machines* (SVM) and *Logistic Regression*.

SVM finds the hyperplane [Equation 1] that best separates the classes' samples. The selected kernel is the linear one that assumes the classes as linearly separable. It was chosen because it provides an easier interpretation than the most common radial basis function kernel. The hyperplane [Equation 1] weight parameter w is derived from the training part of the Support Vector Machines, and the bias factor b_0 is also evaluated.

$$w \cdot x + b_0 = 0 \tag{1}$$

This weights vector w represents the separating hyperplane between the two classes. Therefore, the weight associated with each input gives information about its relevance for the discrimination of the two classes.

The classifier is sensitive to scaling. Thus, the data are standardized through z-scaling to preserve relative spatial distribution, a key element for SVM.

Logistic regression is a statistical technique often used as a classifier since it estimates the probability of an instance belonging to a specific class: if this probability exceeds 50%, the model predicts the instance belonging to the positive class ("1", D in our context); otherwise, it predicts it belongs to the negative class ("0", C). Logistic regression involves computing a weighted sum of input features (along with a bias term) and applying the logistic sigmoid function σ [Equation 2] to the result for binarization of the output.

$$\sigma(t) = \frac{1}{1 + e^{(-t)}} \tag{2}$$

The sigmoid [Equation 2] function outputs a value between 0 and 1.

When fitting a logistic regression model to data, it estimates coefficients for each input feature that indicate the strength and direction of the relationship between that feature and the target variable. It is not mandatory to scale data for Logistic Regression training, but scaling can improve convergence and faster training; therefore, for comparability purposes, the selected scaling for SVM is also applied to logReg input data.

The metric to evaluate the classification quality for both the algorithms is the f1 weighted score, which evaluates independently for each class the f1 score but uses a weight when averaging that depends on the number of samples belonging to each class. The evaluation is done in cross-validation on 5 folds, divided thanks to the stratification technique, which preserves the class ratios among the training and test splits.

For feature importance, the algorithms' coefficients are extracted, and, more specifically, they represent the weights assigned to each input variable for linear SVM and the impact of each feature on the probability estimation for logistic regression. Larger absolute values indicate a stronger influence on the prediction made by the model. By sorting these coefficients in descending order of their absolute values, it is possible to identify which features most impact the predicted outcomes.

TABLE II: p-values for all the features; significant ones highlighted

Feature	P-value
FemCart Density HU Avg	0.770
FemCart Density STD	***5.74E-04***
LatTibCart Density HU Avg	0.110
LatTibCart Density STD	***5.63E-06***
MedTibCart Density HU Avg	***1.74E-02***
MedTibCart Density STD	***4.63E-09***
PatCart Density HU Avg	0.502
PatCart Density STD	***1.50E-05***
FemCart Volume	0.217
LatTibCart Volume	0.138
MedTibCart Volume	***5.81E-08***
PatCart Volume	***1.37E-04***
FemCart Surface	***9.45E-05***
LatTibCart Surface	***7.12E-02***
MedTibCart Surface	***6.82E-03***
PatCart Surface	0.712

III. Results & Discussion

A. Statistical analysis

Table II reports all the p-values computed for each feature, and we can inspect the values by categories (density averages and STDs, cartilage volumes and surfaces) for reducing the dataset. Considering the density averages, only the average of the medial tibial cartilage has a p-value lower than 0.05, enhancing the importance of the medial compartment in knee cartilage degeneration and its higher impact in degeneration [18], [19]. When looking at the STD of these densities, they resulted highly significant for all four cartilages, with p-values significantly lower than 0.05. Moving to geometric features, all the surfaces except the patellar one also resulted significant, but, only medial tibial cartilage and the patellar volume resulted important. Even though the patellar cartilage surface p-value was high, we cannot conclude that the whole cartilage is not determinative in the OA diagnosis because of its volume p-value significance; thus its geometric features need to be taken into account in some measure.

In Fig. 2 it is possible to notice that the pixel density dispersion is always higher in the D class for all four considered cartilages. Cartilage texture parameters show more heterogeneity in OA cartilage, which may precede morphological changes in the progression of OA [20]. The deviation from the mean could be an interesting value for early-stage degeneration. Indeed, when the cartilage degradation is localized on a part of the cartilage, the density can vary among the cartilage itself. However, healthy subjects' density is more constant among the cartilage, as shown in Fig. 2 where the control density STD is always lower than the degenerative ones.

The significant standard density observed in all cartilage during statistical analysis may indicate early-stage degeneration. As suggested by [21], subjects at risk for OA have higher and more heterogeneous knee cartilage MRI T2 values than controls, which are associated with morphologic degeneration.

This may suggest that cartilage density changes in specific regions most affected by the disease but has not yet affected the entire surface. In contrast, in the later stages of degenera-

Authorized licensed use limited to: Reykjavik University. Downloaded on November 23,2026 at 11:59:06 UTC from IEEE Xplore. Restrictions apply.

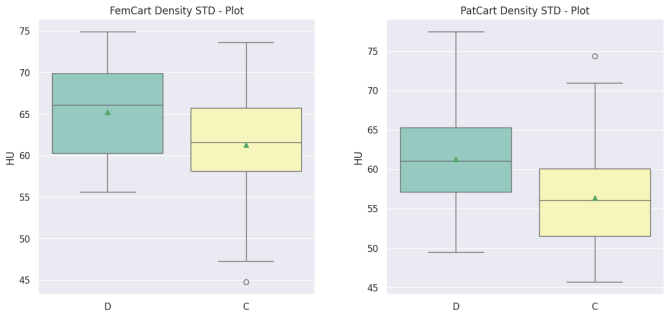

(a) FemCart Density STD

(b) PatCart Density STD

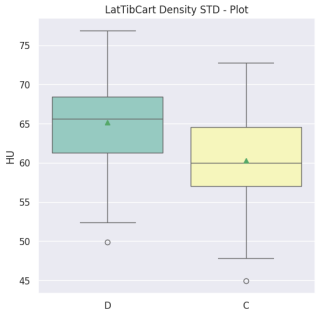

(c) LatTibCart Density STD

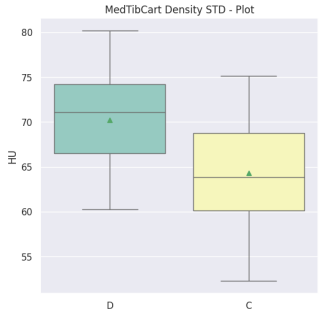

(d) MedTibCart Density STD

Fig. 2: Boxplot of Density STD in HU for all the four considered cartilages in D and C class

tion, the density becomes more uniform as the disease evenly affects the entire cartilage surface.

B. Reduced set of data

Starting from previous considerations, we have decided to reduce the feature set by removing features with less impact on the OA future diagnosis and by creating new features from the existing values.

From the correlation analysis [Fig. 1], both tibialis cartilage volumes and surfaces showed a correlation coefficient of 0.87. Even though the other cartilages do not exhibit high correlation coefficients, they all have been combined for consistency. A new feature, volume-to-surface ratio, has been introduced to replace the use of both volume and surface area separately. This is not a proper feature selection, although reducing dimensionality (even merging features) can improve further analysis. Besides, this measure expresses the compactness and it is proportional to the exposed surface. It can be interpreted as the degeneration status of the deteriorated cartilage. Indeed, as described by Belluzzi *et al.* [22] the changes start from the superficial zone and vertical clefts create, thus changing the volume-surface ratios. Based on the study by Otterness *et al.* [23], there is a correlation between the areas and volumes of knee cartilage in healthy subjects, with a specific constant value describing this relationship for different types of cartilage. However, in our study, which includes both healthy subjects and patients with degenerative conditions, the values for these two groups differ. In patients with degenerative conditions, the relationship between cartilage area and volume may also stabilize to a different constant value after degeneration. This variation can be used to classify the patients, and our results show that this classification is significant, as demonstrated in Table III.

TABLE III: ML results for SVM and Logistic Regression. Average accuracy and STD (in the brackets) among the folds are reported.

	All features	**Reduced features**
Linear SVM	0.81 (0.09)	0.81 (0.03)
Logistic Regression	0.78 (0.09)	0.78 (0.11)

Another interesting correlation result is in cartilage densities: the mean and STD are significantly correlated at more than 0.7 per cartilage. This leads to the possibility of removing the density mean or density STD from the feature set. Since the correlation analysis doesn't provide more information about which feature to choose, we checked their p-values from the statistical data test [Table II]. We have decided to exclude the means from the feature set because the STDs p-values are lower than the mean ones. The decision is substantiated by the understanding, as previously described, that the STD of cartilage density reflects the degree of density variation within the cartilage mask, which can offer more informative insights for degeneration classification.

Therefore, the reduced set of features resulted to be composed as follows:

- FemCart Density STD
- LatTibCart Density STD
- MedTibCart Density STD
- PatCart Density STD
- FemCart Vol/Surf
- LatTibCart Vol/Surf
- MedTibCart Vol/Surf
- PatCart Vol/Surf

In this new dataset, patellar and tibialis cartilages show evident differences [Fig. 3] in values between controls and patients, this is a promising element for the next ML analysis.

C. Machine learning

Both ML algorithms were trained on both the full dataset and the reduced one, and their performances were compared on a 5-fold cross-validation.

Table III reveals minimal performance change between using the full set of features and the reduced set. This indicates that our feature selection approach aligns well with the objectives of our study, as reducing features does not significantly impact model performance. This capability is particularly valuable for diagnostic applications, enabling us to extract fewer features while maintaining high accuracy.

The SVM evaluates features' coefficients during its optimization problem to find the best hyperplane dividing the classes. Indeed, each coefficient corresponds to a feature and represents its relevance in determining the decision boundaries. They are real numbers and factors that multiply the

Authorized licensed use limited to: Reykjavik University. Downloaded on November 23,2026 at 11:59:06 UTC from IEEE Xplore. Restrictions apply.

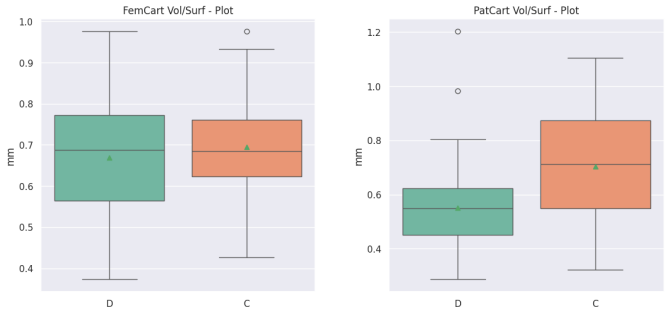

(a) FemCart Volume/Surface (b) PatCart Volume/Surface

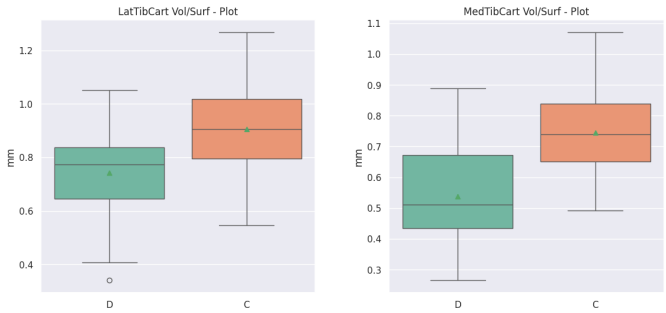

(c) LatTibCart Volume/Surface (d) MedTibCart Volume/Surface

Fig. 3: Boxplot of Volume/Surface for all the four considered cartilages in D and C class

TABLE IV: Coefficients of SVM per feature rounded to three decimal places

Feature	coefficients
LatTibCart Volume	-1.488
MedTibCart Volume	-1.389
LatTibCart Surface	1.074
LatTibCart Density STD	0.738
FemCart Volume	0.656
FemCart Surface	0.574
MedTibCart Surface	0.530
LatTibCart Density HU Avg	-0.504
PatCart Volume	-0.450
PatCart Density HU Avg	-0.432
PatCart Density STD	0.345
FemCart Density HU Avg	-0.275
FemCart Density STD	0.263
MedTibCart Density HU Avg	-0.167
PatCart Surface	-0.143
MedTibCart Density STD	0.0523

corresponding feature value of the sample. Depending on their absolute value and scale, they can give more *importance* to a feature than another one. Thanks to scaling, which reports the values in comparable scales, the coefficients can be compared with each other, ranking the features according to the ML model [Table IV]. The same considerations can be applied to Logistic Regression, even though the performances are slightly less, having its feature ranking in Table V.

In the reduced dataset, as shown in Tables VI and VII, the ratio volume/surface was the most predictive one for all four considered cartilages. In particular, medial tibial cartilage

TABLE V: Coefficients of Logistic Regression per feature rounded to three decimal places

Feature	coefficients
MedTibCart Volume	-1.445
LatTibCart Volume	-1.183
LatTibCart Surface	0.973
PatCart Volume	-0.851
FemCart Surface	0.837
FemCart Volume	0.835
LatTibCart Density STD	0.640
LatTibCart Density HU Avg	-0.572
FemCart Density STD	0.558
MedTibCart Density STD	0.447
PatCart Density STD	0.434
FemCart Density HU Avg	-0.420
MedTibCart Density HU Avg	-0.412
PatCart Density HU Avg	-0.362
MedTibCart Surface	0.314
PatCart Surface	-0.208

TABLE VI: Coefficients of SVM per feature for reduced dataset

Feature	coefficients
MedTibCart Vol/Surf	-1.095
FemCart Vol/Surf	0.879
PatCart Vol/Surf	-0.688
LatTibCart Vol/Surf	-0.683
FemCart Density STD	0.183
LatTibCart Density STD	0.171
MedTibCart Density STD	0.128
PatCart Density STD	-0.010

was the most important. It is also possible to notice that the volume of medial tibial cartilage is the first or the second most predictive in both the algorithms when considering the full set of data (Table IV, Table V). Looking at Table II, it is possible also to notice that all the features related to medial tibial cartilage are significant, and in particular, STD and volume are the ones with the higher p-values in all the datasets. This enhances the importance of looking at the medial compartment for diagnosis purposes.

As enhanced by [18], medial compartment defects progress faster than lateral defects in older adults with minimal to moderate knee OA. [24] also suggested that medial tibiofemoral disease is more common and almost always significant in the development of the disease.

From 3a, results show that there is no big difference between control and degenerative classes on the feature FemCart

TABLE VII: Coefficients of Logistic Regression per feature for reduced dataset

Feature	coefficients
MedTibCart Vol/Surf	-1.336
FemCart Vol/Surf	1.073
PatCart Vol/Surf	-0.823
LatTibCart Vol/Surf	-0.782
FemCart Density STD	0.482
PatCart Density STD	0.198
LatTibCart Density STD	0.126
MedTibCart Density STD	0.080

Authorized licensed use limited to: Reykjavik University. Downloaded on November 23,2026 at 11:59:06 UTC from IEEE Xplore. Restrictions apply.

Volume/Surface. However, looking at Table VI and Table VII, this feature is the second most important for the classification in both tested algorithms. The algorithms evaluate dimensionless coefficients to balance the classification, reflecting the importance relative to the scale of each feature in the specific context of the dataset. It is critical to understand that the importance derived from ML models is not an absolute indicator of the importance of a feature, but rather reflects the optimization process of the model. Therefore, the observed importance of "FemCart Volume/Surface" in the models highlights its role in this analysis and emphasizes the need to interpret ML results within the context of the dataset and algorithm principles.

IV. Conclusions

The precise segmentation aimed to extract meaningful and consistent information from the images, ensuring the accurate representation of cartilage structures within the knee joint. The analysis highlighted the importance of the standard deviation of cartilage density and the medial tibial cartilage as critical indicators of degeneration. The volume-to-surface ratio of cartilage provided valuable insights into morphological changes and disease progression. Both ML models showed robust performance, even with a reduced set of features, indicating that a streamlined approach can maintain high diagnostic accuracy. In conclusion, integrating advanced imaging with ML offers a promising approach to more precise and objective OA diagnosis and monitoring. Future research should focus on refining these methods and validating them in larger patient populations to enhance their clinical utility.

References

[1] A. Litwic, M. H. Edwards, E. M. Dennison, and C. Cooper, "Epidemiology and burden of osteoarthritis," *British Medical Bulletin*, vol. 105, no. 1, pp. 185–199, 01 2013. [Online]. Available: https://doi.org/10.1093/bmb/lds038

[2] Y. Zhang and J. M. Jordan, "Epidemiology of osteoarthritis," *Clinics in Geriatric Medicine*, vol. 26, no. 3, pp. 355–369, 2010, osteoarthritis. [Online]. Available: https://www.sciencedirect.com/science/article/pii/S0749069010000261

[3] T. Neogi, "The epidemiology and impact of pain in osteoarthritis," *Osteoarthritis and Cartilage*, vol. 21, no. 9, pp. 1145–1153, 2013, pain in Osteoarthritis. [Online]. Available: https://www.sciencedirect.com/science/article/pii/S1063458413007607

[4] C. Palazzo, C. Nguyen, M.-M. Lefevre-Colau, F. Rannou, and S. Poiraudeau, "Risk factors and burden of osteoarthritis," *Annals of physical and rehabilitation medicine*, vol. 59, no. 3, pp. 134–138, 2016.

[5] E. M. Roos and N. K. Arden, "Strategies for the prevention of knee osteoarthritis," *Nature Reviews Rheumatology*, vol. 12, no. 2, pp. 92–101, 2016.

[6] L. Murphy, T. A. Schwartz, C. G. Helmick, J. B. Renner, G. Tudor, G. Koch, A. Dragomir, W. D. Kalsbeek, G. Luta, and J. M. Jordan, "Lifetime risk of symptomatic knee osteoarthritis," *Arthritis Care & Research: Official Journal of the American College of Rheumatology*, vol. 59, no. 9, pp. 1207–1213, 2008.

[7] S. Pettenuzzo, A. Arduino, E. Belluzzi, A. Pozzuoli, C. G. Fontanella, P. Ruggieri, V. Salomoni, C. Majorana, and A. Berardo, "Biomechanics of chondrocytes and chondrons in healthy conditions and osteoarthritis: A review of the mechanical characterisations at the microscale," *Biomedicines*, vol. 11, no. 7, 2023. [Online]. Available: https://www.mdpi.com/2227-9059/11/7/1942

[8] E. Ringdahl and S. Pandit, "Treatment of knee osteoarthritis," *American family physician*, vol. 83, no. 11, pp. 1287–1292, 2011.

[9] S. Ahlback, "Osteoarthrosis of the knee. a radiographic investigation," *Acta Radiol Diagn (Suppl)*, vol. 277, pp. 7–72, 1968.

[10] J. H. Kellgren and J. S. Lawrence, "Radiological assessment of osteo-arthrosis," *Annals of the Rheumatic Diseases*, vol. 16, no. 4, pp. 494–502, 1957. [Online]. Available: https://ard.bmj.com/content/16/4/494

[11] C. Ricciardi, H. Jónsson Jr, D. Jacob, G. Improta, M. Recenti, M. K. Gíslason, G. Cesarelli, L. Esposito, V. Minutolo, P. Bifulco *et al.*, "Improving prosthetic selection and predicting bmd from biometric measurements in patients receiving total hip arthroplasty," *Diagnostics*, vol. 10, no. 10, p. 815, 2020.

[12] P. Gargiulo, K. J. Edmunds, M. K. Gíslason, C. Latour, Þ. Hermannsson, L. Esposito, P. Bifulco, M. Cesarelli, M. Fraldi, L. Cristofolini *et al.*, "Patient-specific mobility assessment to monitor recovery after total hip arthroplasty," *Proceedings of the Institution of Mechanical Engineers, Part H: Journal of Engineering in Medicine*, vol. 232, no. 10, pp. 1048–1059, 2018.

[13] M. Recenti, C. Ricciardi, R. Aubonnet, L. Esposito, H. Jónsson, and P. Gargiulo, "A regression approach to assess bone mineral density of patients undergoing total hip arthroplasty through gait analysis," in *2020 IEEE International Symposium on Medical Measurements and Applications (MeMeA)*. IEEE, 2020, pp. 1–6.

[14] M. Binvignat, V. Pedoia, A. J. Butte, K. Louati, D. Klatzmann, F. Berenbaum, E. Mariotti-Ferrandiz, and J. Sellam, "Use of machine learning in osteoarthritis research: a systematic literature review," *RMD Open*, vol. 8, no. 1, 2022. [Online]. Available: https://rmdopen.bmj.com/content/8/1/e001998

[15] F. Ciliberti, L. Guerrini, A. E. Gunnarsson, M. Recenti, D. Jacob, V. Cangiano, Y. A. Tesfahunegn, A. Islind, F. Tortorella, M. Tsirilaki, H. Jónsson, P. Gargiulo, and R. Aubonnet, "Ct- and mri-based 3d reconstruction of knee joint to assess cartilage and bone," *Diagnostics*, vol. 12, 2022.

[16] F. Ciliberti, G. Cesarelli, L. Guerrini, A. E. Gunnarsson, R. Forni, R. Aubonnet, M. Recenti, D. Jacob, H. J. Jr, V. Cangiano, A. Islind, M. Gambacorta, and P. Gargiulo, "The role of bone mineral density and cartilage volume to predict knee cartilage degeneration," *European Journal of Translational Myology*, vol. 32, 2022.

[17] R. Aubonnet, J. Ramos, M. Recenti, D. Jacob, F. Ciliberti, L. Guerrini, M. K. Gislason, O. Sigurjonsson, M. Tsirilaki, H. Jónsson Jr *et al.*, "Toward new assessment of knee cartilage degeneration," *Cartilage*, vol. 14, no. 3, pp. 351–374, 2023.

[18] J. Everhart, M. M. Abouljoud, S. Poland, and D. Flanigan, "Medial compartment defects progress at a more rapid rate than lateral cartilage defects in older adults with minimal to moderate knee osteoarthritis (oa): data from the oa initiative," *Knee Surgery, Sports Traumatology, Arthroscopy*, pp. 1–9, 2018.

[19] G.-Y. Yang, H.-L. Guo, L. T., H. Shang, Y.-F. Zhao, and Y. Shi, "The medial compartment and patellofemoral joint degenerate more severely in early stage knee osteoarthritis: a cross-sectional study." *European review for medical and pharmacological sciences*, vol. 24 19, pp. 9815–9823, 2020.

[20] G. Blumenkrantz, R. Stahl, R. Stahl, J. Carballido-Gamio, S. Zhao, Y. Lu, T. Munoz, M.-P. H. L. Graverand-Gastineau, S. K. Jain, T. Link, and S. Majumdar, "The feasibility of characterizing the spatial distribution of cartilage t(2) using texture analysis." *Osteoarthritis and cartilage*, vol. 16 5, pp. 584–90, 2008.

[21] G. Joseph, T. Baum, J. Carballido-Gamio, L. Nardo, W. Virayavanich, H. Alizai, J. Lynch, C. McCulloch, S. Majumdar, and T. Link, "Texture analysis of cartilage t2 maps: individuals with risk factors for oa have higher and more heterogeneous knee cartilage mr t2 compared to normal controls - data from the osteoarthritis initiative," *Arthritis Research & Therapy*, vol. 13, pp. R153 – R153, 2011.

[22] E. Belluzzi, S. Todros, A. Pozzuoli, P. Ruggieri, E. L. Carniel, and A. Berardo, "Human cartilage biomechanics: Experimental and theoretical approaches towards the identification of mechanical properties in healthy and osteoarthritic conditions," *Processes*, vol. 11, no. 4, 2023. [Online]. Available: https://www.mdpi.com/2227-9717/11/4/1014

[23] I. Otterness, M.-P. Le Graverand, and F. Eckstein, "Allometric relationships between knee cartilage volume, thickness, surface area and body dimensions," *Osteoarthritis and Cartilage*, vol. 16, no. 1, pp. 34–40, 2008. [Online]. Available: https://www.sciencedirect.com/science/article/pii/S1063458407001896

[24] J. C. Stoddart, O. Dandridge, A. Garner, J. Cobb, and R. V. van Arkel, "The compartmental distribution of knee osteoarthritis - a systematic review and meta-analysis." *Osteoarthritis and cartilage*, 2020.

Authorized licensed use limited to: Reykjavik University. Downloaded on November 23,2026 at 11:59:06 UTC from IEEE Xplore. Restrictions apply.